

## Mode conversion between Alfvén and slow waves observed in the magnetotail by THEMIS

J. Du,<sup>1,2</sup> T. L. Zhang,<sup>1</sup> R. Nakamura,<sup>1</sup> C. Wang,<sup>2</sup> W. Baumjohann,<sup>1</sup> A. M. Du,<sup>3</sup> M. Volwerk,<sup>1</sup> K.-H. Glassmeier,<sup>4,5</sup> and J. P. McFadden<sup>6</sup>

Received 9 February 2011; revised 1 March 2011; accepted 7 March 2011; published 6 April 2011.

[1] We present the direct spacecraft observations of wave mode conversion in the magnetotail for the first time. On February 28, 2008, the satellites P4 and P3 of THEMIS observe wave signals with a period of about 100 s in the magnetotail at about 11  $R_E$ . At the same time, geomagnetic activity is very quiet and there are no wave signals observed by the ground-based stations. From P4 observations, Alfvén and slow mode waves are identified during two successive intervals, while the coexistence and slow wave regions are observed by P3. The mode conversion between the Alfvén and slow mode waves takes place while THEMIS are crossing the central current sheet. The sharp curvature of the background magnetic field should be the primary reason of this mode conversion. **Citation:** Du, J., T. L. Zhang, R. Nakamura, C. Wang, W. Baumjohann, A. M. Du, M. Volwerk, K.-H. Glassmeier, and J. P. McFadden (2011), Mode conversion between Alfvén and slow waves observed in the magnetotail by THEMIS, *Geophys. Res. Lett.*, 38, L07101, doi:10.1029/2011GL046989.

### 1. Introduction

[2] The Earth's magnetotail is an extremely complex system, and low frequency waves play an essential role to its dynamics. They can act as an intermediate energy sink or as a carrier to take significant amounts of energy from the magnetotail to the ionosphere, in addition to plasma flows and static field-aligned currents.

[3] Alfvén waves have been observed in many regions of the magnetosphere, and a large number of studies have been performed. *Keiling* [2009] provided a good overview of Alfvén waves and their role in the dynamics of the Earth's magnetotail. In this review spacecraft observations of Alfvén waves from 2000 to 2008 were summarized, organized by region and their three fundamental roles were outlined: energy transport, energy dissipation, and energy sink.

*Glassmeier et al.* [1999] reviewed the observations of field line resonances in different planetary magnetospheres (Earth, Mercury and Saturn), and performed a comparative study which allowed a deeper insight into the critical coupling problem. Based on Cluster data, *Volwerk et al.* [2003, 2004] studied compressional waves in the Earth's neutral sheet.

[4] Because slow mode waves usually suffer heavy Landau damping, there are few spacecraft observations. But the mode conversion between Alfvén and slow waves has been studied in theory and simulation for years. *Southwood and Saunders* [1985], *Walker* [1987], and *Ohtani et al.* [1989] performed some theoretical analysis about waves in a plasma, and suggested that the coupling of the slow and transverse waves could take place in magnetic field configurations involving field-line curvature and intensity inhomogeneity. By investigating the data acquired by the Geotail satellite in the magnetotail from 9 to 30  $R_E$ , *Nakamizo and Iijima* [2003] gave a new perspective on magnetotail disturbances that the substance of Pi2s was the slow magnetohydrodynamic (MHD) waves. They also reported the coexistence and/or coupling of slow and transverse Alfvén waves. But for the data they were using these two types of waves could not be clearly distinguished, and it could be hardly assessed which one was the primary. *Lessard et al.* [2006] reported that the compressional Pi1B pulsations underwent mode conversion to shear Alfvén waves somewhere below the altitude of geosynchronous orbit. Using a one-dimensional model of the magnetotail, *De Keyser* [2000] studied the conversion between different MHD wave modes which could contribute to the observed low-frequency fluctuations in the central plasma sheet (CPS) and plasma sheet boundary layer (PSBL). Low-frequency waves originating in the magnetosheath can transport energy across the tail flank magnetopause and through the tail lobes toward the plasma sheet. In the CPS and PSBL, local conditions permit mode conversion to occur in resonant sheets which can excite Alfvén or slow mode waves. The coupling between the standing shear Alfvén waves (SAW) and slow waves was also studied. During resonance absorption, the ponderomotive force (PF) of SAW can change the local plasma density [*Rankin et al.*, 1995]. The PF-driven density can evolve as slow mode waves [*Tikhonchuk et al.*, 1995; *Rankin and Tikhonchuk*, 1998].

[5] The previous studies about wave mode conversion mainly concentrated on theoretical and simulation analysis. There are a few papers with spacecraft observations [*Southwood and Saunders*, 1985; *Nakamizo and Iijima*, 2003], but instead of direct observations of mode conversion, they only reported fluctuations with mixed transverse and compressional properties. In this paper, direct spacecraft

<sup>1</sup>Space Research Institute, Austrian Academy of Sciences, Graz, Austria.

<sup>2</sup>State Key Laboratory of Space Weather, Center for Space Science and Applied Research, Chinese Academy of Sciences, Beijing, China.

<sup>3</sup>Institute of Geology and Geophysics, Chinese Academy of Sciences, Beijing, China.

<sup>4</sup>Institut für Geophysik und Extraterrestrische Physik, Technische Universität Braunschweig, Braunschweig, Germany.

<sup>5</sup>Max Planck Institute for Solar System Research, Katlenburg-Lindau, Germany.

<sup>6</sup>Space Science Laboratory, University of California, Berkeley, California, USA.

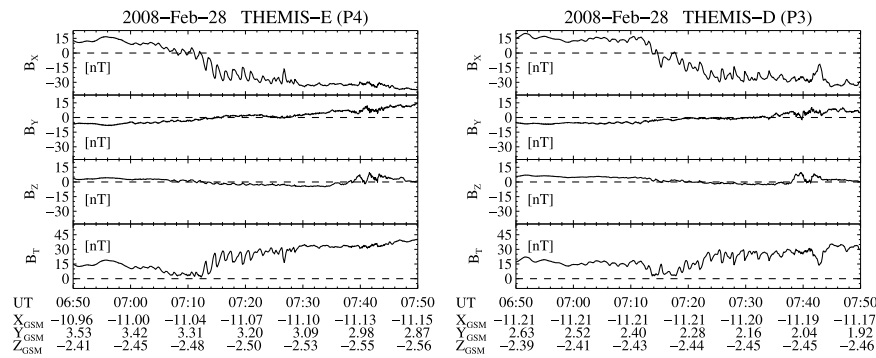


**Figure 1.** Magnetic field data obtained by (left) P4 and (right) P3 from 0650 to 0750 UT on February 28, 2008. Their GSM components are shown in the top three panels respectively, and the magnitude is shown in the bottom panel. The same scale is used to represent the data from P4 and P3. Below each time tick the corresponding positions of probes are given in GSM.

observations of mode conversion in the magnetotail will be presented for the first time.

## 2. THEMIS Observations and Analysis

[6] The data used in our study were obtained by the THEMIS satellites. THEMIS, launched in 2007, consists of five identical satellites [Angelopoulos, 2008]. Each of them is equipped with five in-situ instruments that measure the thermal and super-thermal ions and electrons, and electromagnetic fields from DC to beyond the electron cyclotron frequency. In this study we use spin-fit data (resolution of  $\sim 3$  s) from the Flux Gate Magnetometers (FGM) [Auster *et al.*, 2008] and the Electrostatic Analyzer (ESA) [McFadden *et al.*, 2008].

[7] The event was observed by the two THEMIS probes P4 and P3 from 0650 to 0750 UT on February 28, 2008. The GSM components and the magnitude of magnetic field are shown in Figure 1. All the magnetic components change their direction during this interval. The change of  $B_X$  from positive to negative indicates that the satellites cross the current sheet from the north to south lobe. During this period, P4 made the crossing from  $(-10.96, 3.53, -2.41) R_E$  to  $(-11.15, 2.87, -2.56) R_E$  and P3 moved from  $(-11.21, 2.63, -2.39) R_E$  to  $(-11.17, 1.92, -2.46) R_E$ . The distance between them is about 6000 km. A clear wave signal can be found in the  $B_X$  panel, while the other magnetic components  $B_Y$  and  $B_Z$  have very small fluctuations. Therefore the wave power is mainly concentrated in the  $B_X$  component. The amplitude of this wave increases continuously and then decreases without any sharp change.

[8] In order to analyze the time and frequency properties of the waves, a Morlet wavelet transform is performed on the magnetic field component  $B_X$ . The ion density  $N$  measured by ESA also gives an indication of the wave properties and is processed by the same method. Figure 2 shows the time series and wavelet spectrograms of the magnetic field component  $B_X$  and ion density  $N$ . In the second panel, the fluctuations with a period of about 100 s can be identified from the magnetic field spectrogram. The fluctuations of the magnetic field begin at about 0700 UT for both P4 and P3, and end at about 0730 UT for P4 and 0740 UT for P3. The third panel shows the ion density  $N$ , with its spectra shown in the fourth panel. The typical wave signal

of ion density with a period of about 100 s starts at about 0710 UT for P4 and 0720 UT for P3. An interesting point here is that in spite of the similar frequency magnetic field and ion density start to fluctuate at very different times. As shown in Figure 2, the frequency peaks of fluctuations are at about 0.01 Hz, and the wave powers are mostly concentrated between the two white lines which indicate the time periods 50 s and 150 s respectively.

[9] Figure 3 shows magnetic field variations in the mean field (MF) coordinate, ion pressure variations  $\delta P_i$ , and the angle  $\theta_X$  between the background magnetic field and  $X_{GSM}$  axis. The mean magnetic field are determined by the low-pass filtered data with a shortest period of 150 s. The mean field (MF) coordinate is defined as follows: the principal direction ( $Z_{MF}$  axis) is along the direction of the mean magnetic field, the second direction ( $Y_{MF}$  axis) is perpendicular to the mean magnetic field and  $X$  axis in GSM, and the third direction ( $X_{MF}$  axis) completes the right-handed

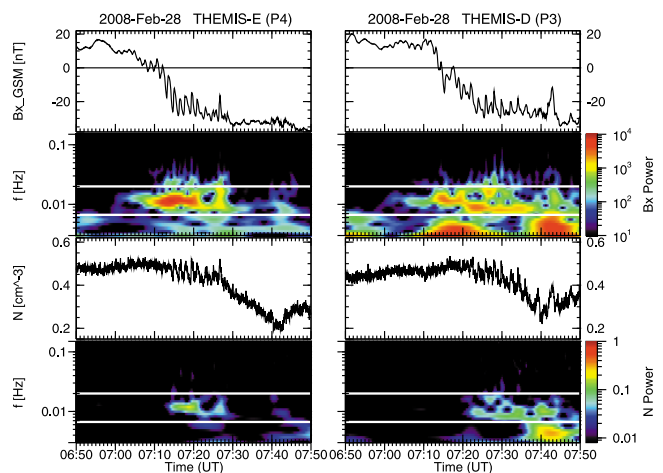


**Figure 2.** From top to bottom: time series of magnetic field component  $B_X$  and its spectrogram, time series of ion density  $N$  and its spectrogram. Two white horizontal lines in spectrogram indicate the time periods 50 and 150 s. The same scale is used to represent the data from (left) P4 and (right) P3.

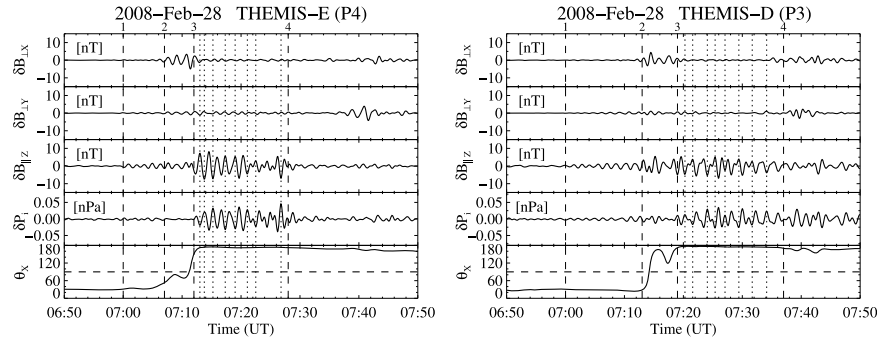


**Figure 3.** From top to bottom: magnetic field variations in the mean field (MF) coordinate, ion pressure variations  $\delta P_i$ , and the angle  $\theta_X$  between the background magnetic field and  $X_{GSM}$  axis. magnetic field and ion pressure data are band-pass filtered with a period of 50 to 150 s. The same scale is used to represent the data from (left) P4 and (right) P3.

coordinated system. The variations of magnetic field and ion pressure are determined by band-pass filtered data with a period of 50 to 150 s, where most of the power of the fluctuations are concentrated as shown in Figure 2. The magnetic field variations are transformed into the MF coordinate system, which allows us to distinguish the transverse ( $\delta B_{\perp X}$  and  $\delta B_{\perp Y}$ ) and compressional ( $\delta B_{\parallel Z}$ ) components of fluctuations.

[10] In Figure 3 four vertical dashed lines, which are marked by the numbers 1–4, indicate four time points 0700, 0710, 0712 and 0728 UT for P4 (0700, 0713, 0719 and 0737 UT for P3), respectively. At 0700 UT, around line 1, the fluctuations of magnetic field start for both of satellites. The amplitudes of magnetic fluctuations are very small and mainly concentrated in the compressional component  $\delta B_{\parallel Z}$  between lines 1 and 2.

[11] The intervals between the lines 2 and 3 for P4 and P3 are discussed in this paragraph. As shown in Figure 3 (left) for P4, the transverse component  $\delta B_{\perp X}$  of the magnetic fluctuations is dominant and the ion pressure remains very quiet. This indicates that the waves observed by P4 during this interval should be Alfvén mode.  $\theta_X$  is close to  $90^\circ$  at the same time, so the background field is nearly perpendicular to  $X_{GSM}$  axis and P4 is crossing the current sheet. In Figure 3 (right), P3 crosses the current sheet from 0713 to 0719 UT (the lines 2 and 3) when  $\theta_X$  changes from  $30^\circ$  to  $180^\circ$ . Although the transverse component  $\delta B_{\perp X}$  of the magnetic fluctuations is still less than the compressional component  $\delta B_{\parallel Z}$ , the former gets larger at 0713 UT (line 2) and becomes comparable to the latter. The magnetic fluctuations have both the transverse and compressional components. Moreover, ion pressure also have some small variations which is out-of-phase with the compressional component  $\delta B_{\parallel Z}$ . It indicates that the coexistence of Alfvén and slow mode waves is observed by P3 during this interval.

[12] In Figure 3, the fluctuations of ion pressure become significant at 0712 UT for P4 and 0719 UT for P3, which is marked by line 3. At the same time, the compressional component  $\delta B_{\parallel Z}$  of magnetic fluctuations are strengthened remarkably and the transverse components almost disappear. The background field is anti-parallel to  $X_{GSM}$  axis with  $\theta_X$  close to  $180^\circ$  between the lines 3 and 4 (0712–0728 UT for P4; 0719–0737 UT for P3). Some dotted lines are drawn to show that  $\delta B_{\parallel Z}$  and  $\delta P_i$  vary exactly out-of-phase. This

indicates that the fluctuations during this interval exhibit the property of slow or mirror mode waves. During this time interval the temperature is nearly isotropic which cannot excite the mirror mode instability. Although the velocities of plasma flow observed by P4 and P3 are distinctly different, the primary frequencies of fluctuations are close to each other. It indicates that the fluctuations cannot be the mirror mode structures which are static in the plasma flow, and should be the slow mode waves.

[13] In summary, there are three kinds of regions with the different wave modes: pure Alfvén mode region between the lines 2 and 3 observed by P4; coexistence of Alfvén and slow modes region between the lines 2 and 3 observed by P3; pure slow mode region between the lines 3 and 4 observed by both P4 and P3. The mode conversion is clearly observed at about 0712 UT by P4 and 0719 UT by P3. This is the first direct observation of mode conversion in the Earth’s magnetotail.

### 3. Discussion

[14] On February 28, 2008, waves with a period of about 100 s are observed by P4 and P3 in the magnetotail at about 11  $R_E$ . The magnetic field start to fluctuate at 0700 UT, while the fluctuations of ion pressure begin at 0712 UT for P4 and become significant at 0719 UT for P3. Alfvén mode waves are identified from the observations of P4 during 0707–0712 UT, and slow mode waves are observed by both P4 and P3 (0712–0728 UT for P4; 0719–0737 UT for P3). The coexistence region of Alfvén and slow waves is observed by P3 from 0707 to 0712 UT. There is a clear mode conversion from Alfvén to slow mode waves at about 0712 UT for P4 and 0719 UT for P3.

[15] The averages of magnetic field and plasma parameters for three kinds of regions are given in Table 1. The average plasma moments measured by ESA such as ion velocity, density and temperature change very little for the different regions. The major difference is that the average magnetic field is weak and nearly perpendicular to  $X_{GSM}$  axis in Alfvén wave region, while it is strong and anti-parallel to  $X_{GSM}$  axis in slow wave region. It results in the significant differences in plasma  $\beta$  and  $\theta_X$ . The averages of magnetic field and plasma parameters in coexistence region lie in between the values in Alfvén and slow wave regions.

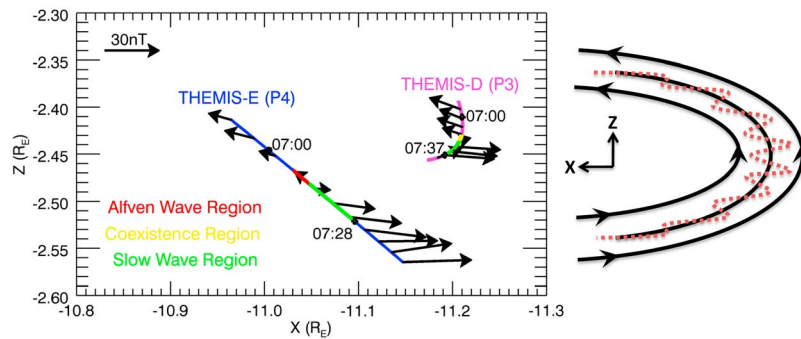


**Figure 4.** (left) The orbits of P4 (blue line) and P3 (green line) with the magnetic vectors (black arrows) from 0650 to 0750 UT on February 28, 2008 in GSM. Red and yellow parts mark the Alfvén and slow wave regions, respectively. (right) Schematic illustration of the mode conversion is shown. Black lines indicate the background magnetic field and dark red dash line represent the fluctuations of magnetic field.

Figure 4 shows the orbits of P4 (blue line) and P3 (purple line) with the magnetic vectors (black arrows) from 0650 to 0750 UT on February 28, 2008 in GSM. Alfvén, coexistence and slow wave regions are highlighted by red, yellow and green lines, respectively. Alfvén wave region is close to the current sheet, and the magnetic vector is very short which indicates that the background field is almost along  $Y_{GSM}$  axis. In coexistence region, the magnetic field have a small negative  $B_X$  component and is oblique to  $X_{GSM}$  axis. Slow wave region have a strong background field which almost points to the negative  $X_{GSM}$  direction. It is clear that the mode conversion occurs while the satellites are crossing the current sheet from north to south. This is in agreement with the theoretical results of *Southwood and Saunders* [1985]. They find that the coupling of slow and Alfvén waves can occur where field lines are sharply bent as for instance they are near the equator in the terrestrial magnetotail. *De Keyser* [2000] developed a nonstatic linear MHD model to examine the propagation of waves for frequencies from 5 to 50 mHz. He found that in the CPS and PSBL, mode conversion can excite Alfvén or slow waves in thin resonant sheets. In our study, the ion density remains at about  $0.45 \text{ cm}^{-3}$  for each region, which indicates that the satellites are still in the CPS. The direction of the magnetic fluctuations has very little change over the different regions and stays nearly along  $X_{GSM}$  axis, as seen in Figure 1. The conversion between transverse and compressional waves is due to the change of direction of the background magnetic field. As shown in Figure 3, when the background field is perpendicular to  $X_{GSM}$  axis, the transverse component of magnetic field is dominant and the waves are identified as Alfvén mode. When the background field is anti-parallel to

$X_{GSM}$  axis with the  $\theta_X$  close to  $180^\circ$ , the magnetic fluctuations are compressional and exactly out-of-phase with ion pressure variations, which is the property of slow mode waves. When the background field is oblique to  $X_{GSM}$  axis, Alfvén and slow mode waves coexist. A simple schematic illustration of the mode conversion is shown in Figure 4 (right). Dark red line represents the magnetic fluctuations along  $X$ . When the background field direction changes, the transverse and compressional components of waves can change into each other.

[16] In order to study the origin and propagation of the waves, we investigate the simultaneous upstream and ground based observations. Although the other three probes of THEMIS are also in the magnetotail, they do not observe the same wave signals as P4 and P3. The waves may be restricted in thin resonant sheets. At the same time, low AE and DST index indicate that the geomagnetic activity is very low. The simultaneous ground based observations do not show any waves either. This is probably because slow mode waves are heavily Landau damped and dissipate in the magnetotail. CLUSTER is just in front of the bow shock during the time period, which can monitor the change of solar wind. Apart from a small southward magnetic field (negative  $B_Z$ ) near 0700 UT, it observes no noticeable change of the solar wind condition. In the magnetotail, none of the THEMIS probes observes any high speed flow. The local temperature is almost isotropic, which cannot satisfy any instabilities to excite the waves. The waves observed by P4 and P3 should be generated at other places. The Kelvin-Helmholtz instability at the boundary layer and waves in the magnetosheath are possible sources [*Southwood and Saunders*, 1985; *De Keyser*, 2000; *Guo et al.*, 2010].

**Table 1.** Background Magnetic Field and Plasma Parameters in Each Region of February 28, 2008 Observed by P4 and P3

	Alfvén Wave Region P4 (0707–0712 UT)	Coexistence Region P3 (0713–0719 UT)	Slow Wave Region	
			P4 (0712–0728 UT)	P3 (0719–0737 UT)
Magnetic Field [nT]	(0.69, -3.25, 1.10)	(-3.12, -2.56, 1.42)	(-22.12, 0.91, -2.25)	(-22.12, -0.16, -1.39)
Ion Velocity [km/s]	(16.05, 37.75, 5.43)	(26.15, 50.85, 10.63)	(16.08, 47.29, 3.68)	(18.31, 65.66, 9.31)
Ion Density [ $\text{cm}^{-3}$ ]	0.49	0.48	0.46	0.44
Ion Temperature [keV]	4.45	4.33	4.01	3.75
Plasma $\beta$	43.95	18.66	1.47	1.34
$\theta_X$ [°]	79	137	173	176

[17] **Acknowledgments.** This work in China was supported by the Specialized Research Fund for State Key Laboratories, the Knowledge Innovation Program of the Chinese Academy of Sciences, Chinese Academy of Sciences grant KJCX2-YW-T13 and the National Science Foundation of China (NSFC) grants 41004078 and 40921063. The work by KHG is financially supported by the German Ministerium für Wirtschaft und Technologie and the Deutsches Zentrum für Luft- und Raumfahrt under grant 50OC1001. We acknowledge NASA contract NAS5-02009 for use of data from the THEMIS mission.

[18] The Editor thanks Robert Rankin and an anonymous reviewer for their assistance in evaluating this paper.

## References

- Angelopoulos, V. (2008), The THEMIS mission, *Space Sci. Rev.*, *141*(1–4), 5–34, doi:10.1007/s11214-008-9336-1.
- Auster, H. U., et al. (2008), The THEMIS fluxgate magnetometer, *Space Sci. Rev.*, *141*(1–4), 235–264, doi:10.1007/s11214-008-9365-9.
- De Keyser, J. (2000), Magnetohydrodynamic wave mode conversion in the Earth's magnetotail, *J. Geophys. Res.*, *105*(A6), 13,009–13,016, doi:10.1029/2000JA900020.
- Glassmeier, K.-H., C. Othmer, R. Cramm, M. Stellmacher, and M. Engebretson (1999), Magnetospheric field line resonances: A comparative planetology approach, *Surv. Geophys.*, *20*(1), 61–109, doi:10.1023/A:1006659717963.
- Guo, X. C., C. Wang, and Y. Q. Hu (2010), Global MHD simulation of the Kelvin-Helmholtz instability at the magnetopause for northward interplanetary magnetic field, *J. Geophys. Res.*, *115*, A10218, doi:10.1029/2009JA015193.
- Keiling, A. (2009), Alfvén waves and their roles in the dynamics of the Earth's magnetotail: A review, *Space Sci. Rev.*, *142*(1–4), 73–156, doi:10.1007/s11214-008-9463-8.
- Lessard, M. R., E. J. Lund, S. L. Jones, R. L. Arnoldy, J. L. Posch, M. J. Engebretson, and K. Hayashi (2006), Nature of Pi1B pulsations as inferred from ground and satellite observations, *Geophys. Res. Lett.*, *33*, L14108, doi:10.1029/2006GL026411.
- McFadden, J. P., C. W. Carlson, D. Larson, M. Ludlam, R. Abiad, B. Elliott, P. Turin, M. Marckwordt, and V. Angelopoulos (2008), The THEMIS ESA plasma instrument and in-flight calibration, *Space Sci. Rev.*, *141*(1–4), 277–302, doi:10.1007/s11214-008-9440-2.
- Nakamizo, A., and T. Iijima (2003), A new perspective on magnetotail disturbances in terms of inherent diamagnetic processes, *J. Geophys. Res.*, *108*(A7), 1286, doi:10.1029/2002JA009400.
- Ohtani, S., A. Miura, and T. Tamao (1989), Coupling between Alfvén and slow magnetosonic waves in an inhomogeneous finite-beta plasma—I. Coupled equations and physical mechanism, *Planet. Space Sci.*, *37*(5), 567–577, doi:10.1016/0032-0633(89)90097-4.
- Rankin, R., and V. T. Tikhonchuk (1998), Numerical simulations and simplified models of nonlinear electron inertial Alfvén waves, *J. Geophys. Res.*, *103*(A9), 20,419–20,433, doi:10.1029/98JA01186.
- Rankin, R., P. Frycz, V. T. Tikhonchuk, and J. C. Samson (1995), Ponderomotive saturation of magnetospheric field line resonances, *Geophys. Res. Lett.*, *22*(13), 1741–1744, doi:10.1029/95GL01311.
- Southwood, D. J., and M. A. Saunders (1985), Curvature coupling of slow and Alfvén MHD waves in a magnetotail field configuration, *Planet. Space Sci.*, *33*(1), 127–134, doi:10.1016/0032-0633(85)90149-7.
- Tikhonchuk, V. T., R. Rankin, P. Frycz, and J. C. Samson (1995), Nonlinear dynamics of standing shear Alfvén waves, *Phys. Plasmas*, *2*(2), 501–515, doi:10.1063/1.870975.
- Volwerk, M., et al. (2003), A statistical study of compressional waves in the tail current sheet, *J. Geophys. Res.*, *108*(A12), 1429, doi:10.1029/2003JA010155.
- Volwerk, M., et al. (2004), Compressional waves in the Earth's neutral sheet, *Ann. Geophys.*, *22*(1), 303–315, doi:10.5194/angeo-22-303-2004.
- Walker, A. D. M. (1987), Theory of magnetospheric standing hydromagnetic waves with large azimuthal wave number 1. Coupled magnetosonic and Alfvén waves, *J. Geophys. Res.*, *92*(A9), 10,039–10,045, doi:10.1029/JA092iA09p10039.

A. M. Du, Institute of Geology and Geophysics, Chinese Academy of Sciences, Dewai Street, Beijing 100029, China.

W. Baumjohann, J. Du, R. Nakamura, M. Volwerk, and T. L. Zhang, Space Research Institute, Austrian Academy of Sciences, Schmiedlstr. 6, A-8042 Graz, Austria. (jdu@spaceweather.ac.cn)

K.-H. Glassmeier, Institut für Geophysik und Extraterrestrische Physik, Technische Universität Braunschweig, Mendelssohnstr. 3, D-38106 Braunschweig, Germany.

J. P. McFadden, Space Science Laboratory, University of California, 7 Gauss Way, Berkeley, CA 94720, USA.

C. Wang, State Key Laboratory of Space Weather, Center for Space Science and Applied Research, Chinese Academy of Sciences, PO Box 8701, Beijing 100190, China.